Hindawi
Mobile Information Systems
Volume 2022, Article ID 1359472, 14 pages
https://doi.org/10.1155/2022/1359472

Research Article

Hierarchical Lattice Modeling Method with Gradient Functions

Cheng Cheng,[1] **Ning Dai**,[2] **Weiping Gu**,[3] **Bai Xu**,[1] **and Jing Xu**[1]

[1]*College of Aeronautical Engineering, Nanjing Vocational University of Industry Technology, Nanjing, Jiangsu 210046, China*
[2]*College of Mechanical and Electrical Engineering, Nanjing University of Aeronautics and Astronautics, Nanjing, Jiangsu 210016, China*
[3]*The Affiliated Stomatological Hospital of Nanjing Medical University, Nanjing, Jiangsu 210029, China*

Correspondence should be addressed to Cheng Cheng; 19413118@smail.cczu.edu.cn

Received 31 March 2022; Revised 13 May 2022; Accepted 19 May 2022; Published 1 June 2022

Academic Editor: Abid Yahya

Lattice structure materials have great application potential in biomedical, aerospace, and other fields. In fact, designing multilevel structure parametrically to achieve excellent mechanical performance is a challenging task. In this paper, a hierarchical lattice modeling method with gradient functions is proposed on the basis of the multilevel structural characteristics of organisms to solve the problem of the coexistence of high hardness, high strength, and high toughness. The multilevel body space is filled with matching lattices in accordance with the given dynamic parameters, and the design is optimized in accordance with the simulation results. Thus, the desired composite functional structure is generated. In fact, the proposed method is divided into two stages, that is, preprocessing and design. In the former stage, the interpolation method is used to establish a lattice unit model family retrieved by parameters, such as elastic modulus and impact toughness. In the latter stage, the multilevel 3D reconstruction model is initially filled with the gradient multilevel lattices through the global optimization technique with an isosurface modeling algorithm. The porosity, rod diameter, and other parameters of the lattice structure are regulated in accordance with the results of finite element analysis through image mapping, meeting the requirements of biomechanical characteristics. Our empirical evaluation and experimental results demonstrate that the proposed method can control the relationship between porous structure porosity, elastic modulus, and impact toughness and design bionic multispace microstructures close to biodental displacement and deformation.

1. Introduction

Lattice structural materials are potential lightweight multifunctional structural materials with better mechanical properties than the conventional materials. Lattice structure materials have great application potential in biomedical, aerospace, and other fields of the real life. Furthermore, the development of additive manufacturing ensures the manufacturing of lattice structures. In fact, creatures in nature have evolved over tens of thousands of years and gradually developed unique structural and mechanical properties. These properties allow them to function beyond the man-made systems through using their complex multiscale and multiphase structures [1–5]. These multilayer biostructure materials tend to have more reasonable mechanical properties than single structural materials. The teeth, bones, and pearls of common multilevel organisms are taken as examples [6]. These biostructure materials have excellent mechanical properties, such as hard surface layers to resist wear or penetration and tough internal structures to adapt to deformation. These characteristics are closely related to the multilevel structure within the organism. However, designing multilevel structure parametrically to achieve excellent mechanical performance is still challenging.

In this study, multilevel organisms are taken as the main research objects, and their tenacity principle is explored from the microlevel. A lattice model family with lattice porosity driving the dynamic performance regulation is constructed, and the filling of the target object is optimized. On the basis of finite element mapping, the lattice showed gradient changes so as to be close to the structural gradient

change characteristics maximally. The transition connection between lattices is optimized on the basis of the implicit surface method, thereby ensuring the effectiveness of the connection between the structures and the steady transition of forces. Through empirical evaluation, iterative optimization results, in models, were obtained with robust shape structures that meet the tenacity of biomechanical properties. In addition, the control method of multilevel lattice mechanical performance was also evaluated and applied to the biological model through combining and amalgamating physical experiments with simulation experiments. Experimental results show that the proposed method can control the relationship between porous structure porosity, elastic modulus, and impact toughness and design bionic multispace microstructures close to biodental displacement and deformation. The major contributions of the research conducted in this paper are described as follows:

(i) A hierarchical lattice modeling method with gradient functions is proposed on the basis of the multilevel structural characteristics of organisms to solve the problem of the coexistence of high hardness, high strength, and high toughness.

(ii) A lattice model family with lattice porosity driving the dynamic performance regulation is constructed, and the filling of target object is optimized.

(iii) The proposed method is divided into two stages, that is, preprocessing and design. In the former one, the interpolation method is used to establish a lattice unit model family retrieved by parameters. In the latter one, the multilevel 3D reconstruction model is initially filled with the gradient multilevel lattices through global optimization with an isosurface modeling algorithm.

The remaining of this is structured as follows. In Section 2, we offer a review and brief summaries of various state-of-the-art related works. In Section 3, we discuss the technical protocol and design. In Section 4, the lattice structure design is illustrated. In Section 5, we discuss the realization of multilevel microstructure filling. Experimental results and analysis are discussed in Section 6. Multilevel bionic microstructure design and review of the related works are elaborated in Section 7. Finally, Section 8 concludes this paper and offers several directions and opportunities for further research and investigation.

2. Related Work

The lattice structure materials have great application potential in biomedical, aerospace, and other fields. In fact, designing multilevel structure parametrically to achieve excellent mechanical performance is a challenging task. Many authors have conducted studies on the mechanical properties of unit structures. Zhang et al. [7] proposed a topological optimization method for designing composite damping materials that work over a wide range of vibration frequencies. A mathematical model with K–S target function and weighted target function is established. This model is used to find the optimal two-phase damping material layout on the microscale so that an effective complex elastic matrix of homogeneity is obtained. Dong et al. [8] extended the topological optimization of coating materials to multi-gradient structures. In the process of modeling biological bones, three different levels of density gradients are defined, and the periosteum and compact bone are separated by using modified nonmonotonic filter functions. Their outcomes demonstrate the superiority of the proposed method.

Shimoda et al. [9] expressed the simultaneous optimization problem of shape and topology as the distribution parameter optimization for nonparametric shape topology optimization of multimaterial frame structures. They used the Lagrangian multiplier method, material derivative method, and adjoint variable method to derive the shape gradient function and material gradient function to optimize the design. He et al. [10] established a multimaterial interpolation value model, improved the mathematical planning algorithm based on gradients by using the adjoint variable method, and considered the additional constraints of structure retention in the design. Alacoque et al. [11] proposed a regional scale aggregation stress constraint method and developed a topological optimization framework to synthesize high-strength spatial periodic materials with unique thermal elasticity by using homogenized thermal stress and mechanical stress analysis formula. Jia et al. [12] achieved the aperiodicity of local structures by using a k-mean clustering algorithm and unit strain energy and established a heterogeneous structure optimization model with nonuniform lattices on the microscale [12]. The use of the k-mean clustering technique enables the proposed approach to demonstrate its applicability.

At present, various optimization solutions have been proposed for periodic mesoscale unit structure design. However, designers must consider homogenization; that is, the size of a single cell must be smaller than the design space in all directions. Assuming that the lattice structure is periodic in all directions, the elastic modulus of the lattice unit can be calculated by homogenization. The microstructure connection of various materials has received extensive attention. Woischwill et al. [13] used gradient-based optimization techniques to decompose multimaterial design optimization problems into an optimal topology for multiple material structures and optimal designs for multiple joint types. Under the mass fraction constraint, Florea et al. [14] proposed an algorithm to determine the optimal location and selection of nonconnected materials and intercomponent jointing materials. Luo et al. [15] presented a multiscale multiobjective optimization method based on self-connecting material interpolation. This method defines the interface area between different microstructures and deals with structural topology optimization problems with multiple different but connected microstructures. Liu et al. [16] used density models to represent microstructure topology and introduced predefined connection areas that share the same topology to design structures consisting of repeating units and lattice materials that specify porosity.

3. Technical Protocol

The multilevel body space was filled with matching lattices in accordance with the given dynamic parameters. The design was optimized in accordance with the simulation results to form the desired composite functional structure. The method is divided into two stages. In the preprocessing stage, the interpolation method was used in finite element simulation to establish a lattice unit model family retrieved by parameters, such as elastic modulus and impact toughness. During the design process, the resulting biocomputed tomography (CT) image was first reconstructed to obtain multilevel body space. On the basis of the results on the mechanical performance of organisms at all levels, the biodynamic parameters of all levels were entered to match the unit structure in the lattice model family. In accordance with the given dynamic parameters, the model space at all levels was filled, the model was initially optimized by the global optimization method, and the validity and stability of the connection were guaranteed.

The model was then imported into finite element analysis. The model was analyzed in accordance with the actual force condition, and the mechanical results of the model were exported. The analysis results were matched with the lattice filling model through 3D mapping so as to adjust the porosity, size, and other parameters of the lattice structure. The optimized results were reimported into finite elements for analysis in order to authenticate and verify that the need for biological deformation was successfully met. If not satisfied, return to complete the optimization process again iteratively until a model with a robust shape structure and biomedical characteristics is generated. The flowchart of the proposed lattice structure is shown in Figure 1.

4. Lattice Structure Design

4.1. Homogenization. At present, various optimization solutions have been proposed for periodic mesoscale unit structure design. However, designers must consider homogenization; that is, the size of a single cell must be smaller than the design space in all directions. Assuming that the lattice structure is periodic in all directions, the elastic modulus of the lattice unit can be calculated by homogenization. The stiffness matrix consisting of lattice units M can be expressed as given by equation

$$M = \sum_{i=1}^{n} \int_{\Omega_i} R^T C_i R \mathrm{d}\Omega_i, \tag{1}$$

where n is the number of lattice unit grids; R is the stress-strain matrix; C_i is the matrix used to represent the crystal lattice related to the cell density; and Ω_i is the ith unit domain.

The lattice unit is denoted as c. The load in six directions needs to be solved to calculate the structural characteristics of the lattice unit.

$$MX^{(i)} = F^{(i)}, \quad i = 1, 2, \ldots, 6, \tag{2}$$

where $X^{(i)}$ is the displacement vector of each lattice unit c in the direction of i and $F^{(i)}$ is the applied load, which can be calculated by the stress field.

$$F^{(i)} = \sum_{i} \int_{\Omega_i} R^T C_i \varepsilon^{(i)} \mathrm{d}\Omega_i. \tag{3}$$

The unit strain matrix is computed as given in the following:

$$\begin{aligned}
\varepsilon^{(1)} &= \begin{bmatrix} 1 & 0 & 0 & 0 & 0 & 0 \end{bmatrix}^T, \\
\varepsilon^{(2)} &= \begin{bmatrix} 0 & 1 & 0 & 0 & 0 & 0 \end{bmatrix}^T, \\
\varepsilon^{(3)} &= \begin{bmatrix} 0 & 0 & 1 & 0 & 0 & 0 \end{bmatrix}^T, \\
\varepsilon^{(4)} &= \begin{bmatrix} 0 & 0 & 0 & 1 & 0 & 0 \end{bmatrix}^T, \\
\varepsilon^{(5)} &= \begin{bmatrix} 0 & 0 & 0 & 0 & 1 & 0 \end{bmatrix}^T, \\
\varepsilon^{(6)} &= \begin{bmatrix} 0 & 0 & 0 & 0 & 0 & 1 \end{bmatrix}^T.
\end{aligned} \tag{4}$$

4.2. Construction of the Lattice Model Family. On the basis of homogenization theory, the design of lattice units was conducted, and several common lattice unit structures were observed, as shown in Figure 2. The strategy of precomputation was adopted to efficiently and accurately retrieve microstructures with specific parameters. Considering the connection between lattice units, the lattice unit structure was divided into four categories, namely, face-centered cubic (FCC), body-centered cubic (BCC), face and body-centered cubic (FBCC), and rhombic dodecahedron (RD), to ensure that adjacent structures can be connected steadily. The finite element analysis of each lattice structure was then conducted to obtain the corresponding dynamic parameters of different lattice structures. The corresponding parameter information, such as lattice category, porosity, impact toughness, and elastic modulus, was given to the constructed unit structures to establish the mapping relationship between the lattice and the parameters. A set of elastic modulus corresponding to the lattice unit driven by the porosity can be obtained by regulating the porosity of the lattices. A set of continuous lattice model systems can be achieved by interpolating this set of data [16]. The distance field conversion function is utilized to transform the model space.

$$f(x) = \mathrm{sgn}(x) \ln(|x| + \delta), \tag{5}$$

where δ is the threshold for adjusting the fitting accuracy. The smaller the value of δ is, the higher the fitting accuracy. In accordance with the given porosity φ_{goal} and transformation distance field $f(x)$, linear interpolation with the least square method is used to solve ξ.

$$\xi = \min_{f \in \Pi_m^d} \sum_{i} f(x_i) c_{\mathrm{base}} - f\left(\varphi_{\mathrm{goal}}\right)^2, \tag{6}$$

where d is the space dimensionality; m is the degree of the polynomial; x_i is the ith value of x; and Π is the domain of all lattices. When ξ is the smallest, then φ_{goal} can be obtained. The

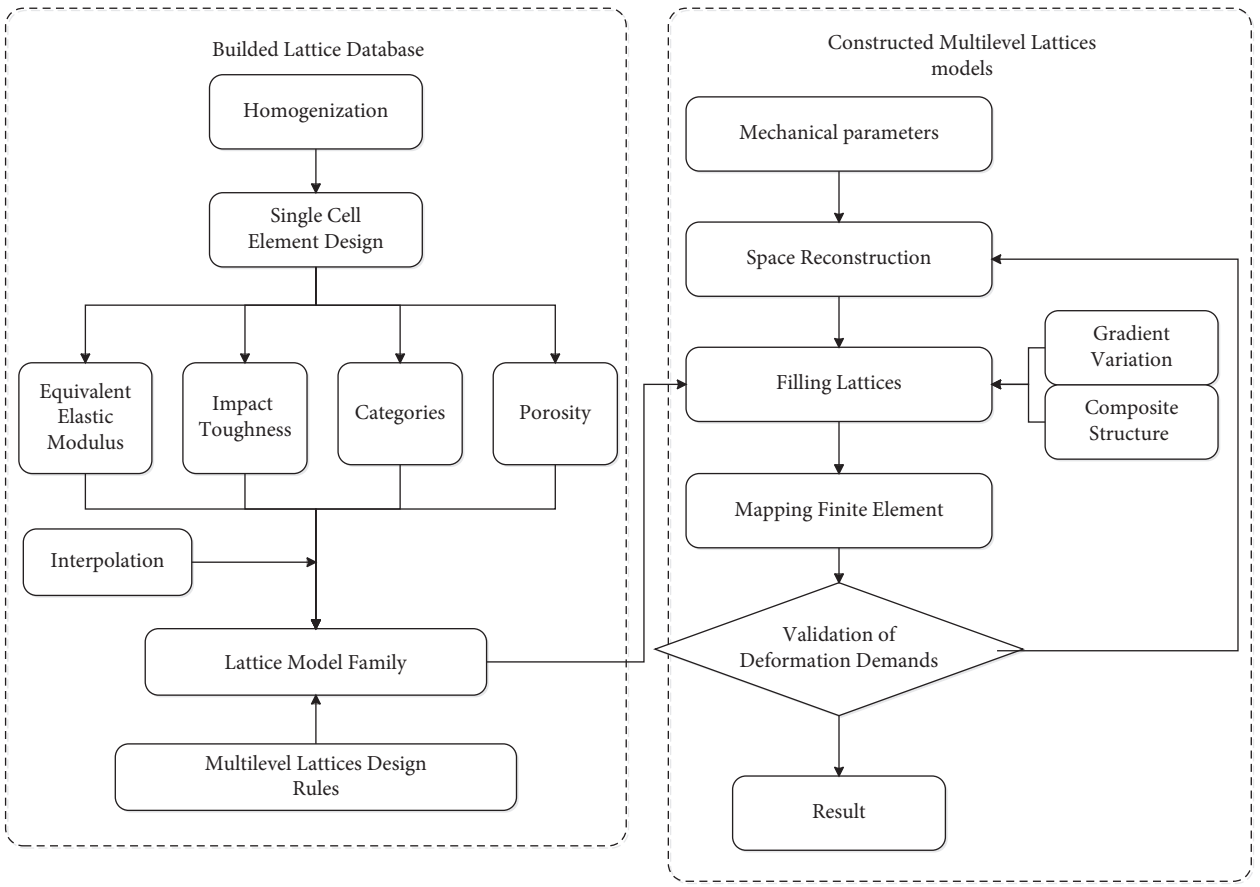

Figure 1: The flowchart of modeling lattice structure with gradient functions.

corresponding unit volume structure c_{goal} can be obtained through interpolation calculation of the basic unit c_{base}.

In this way, a more accurate lattice family can be obtained. It should be noted that the applicability and accuracy of the proposed method can be improved further through continuously increasing the lattice types to provide rich initial samples for the selection of multilevel parameter mechanical performance control. Figure 3 shows the change trend of four typical lattice structures (BCC, FCC, FBCC, and RD) and five typical structural elastic modules driven by porosity. As shown in the mechanics test, the elastic modulus corresponding to the lattice structure with different porosities is linearly distributed. When the unit model family database is perfect, then more lattice cells are selected for modeling, making the design of multilevel models easy with more personalized requirements [17].

4.3. Multilevel Lattice Unit Mechanics Control Method. On the basis of the theoretical research of the unit lattice, the mechanics control method of the multilevel lattice structure was proposed. Fundamentally, this method can be traced back to the law of linear elasticity: $\sigma = E\varepsilon$, where $\sigma = \{\sigma_1, \sigma_2, \sigma_3, \sigma_4, \sigma_5, \sigma_6\}$ and $\varepsilon = \{\varepsilon_1, \varepsilon_2, \varepsilon_3, \gamma_4, \gamma_5, \gamma_6\}$. The mean calculation method of the lattice unit is defined. The lattice unit is extended to a single-level lattice model, the number of m single-level lattice layers is defined, and n is the number of m-level lattices [18]. The single-level lattice elastic modulus is represented by homogenization theory as given by equation

$$E_{ij}^{H} = \sum_{e=1}^{mn} Q_{ij}^{e} = \sum_{e=1}^{mn} \left[\frac{1}{Y_e} \int_{Y_e} \mathbf{E}\left(\left(\boldsymbol{\varepsilon}_i^0\right)^{\mathrm{T}} - \boldsymbol{\varepsilon}_i^{\mathrm{T}} \right) \cdot \left(\boldsymbol{\varepsilon}_j^0 - \boldsymbol{\varepsilon}_j \right) dY_e \right] i, \quad (7)$$

$j = 1, 2, \ldots, 6,$

where E is the elastic modulus of the lattice unit; Y_e is the variable related to e; ε_i^0 and ε_j^0 are the actual strain fields of the i and j elements; and ε_i and ε_j denote the corresponding theoretical strain fields, respectively.

E_{ij}^{H} is obtained on the basis of six different constraints and force application methods, and the elastic matrix E^H of 6×6 is composed of E_{ij}^{H}. Considering that the boundary connection problems are likely to occur between the levels, the function is adopted for definition and is given by the following equation:

$$\xi_{(i,j),(m,n)} = \exp\left(d_{(i,j),(m,n)} \cdot g_{(i,j),(m,n)} \right). \quad (8)$$

The matching degree between the jth lattice unit in the ith layer and the nth lattice unit in the mth layer is described. $d_{(i,j),(m,n)}$ is the connection error between the selected structure and the actual microstructure, and $g_{(i,j),(m,n)}$ is the similarity between adjacent structures. The multilevel structure is then defined as

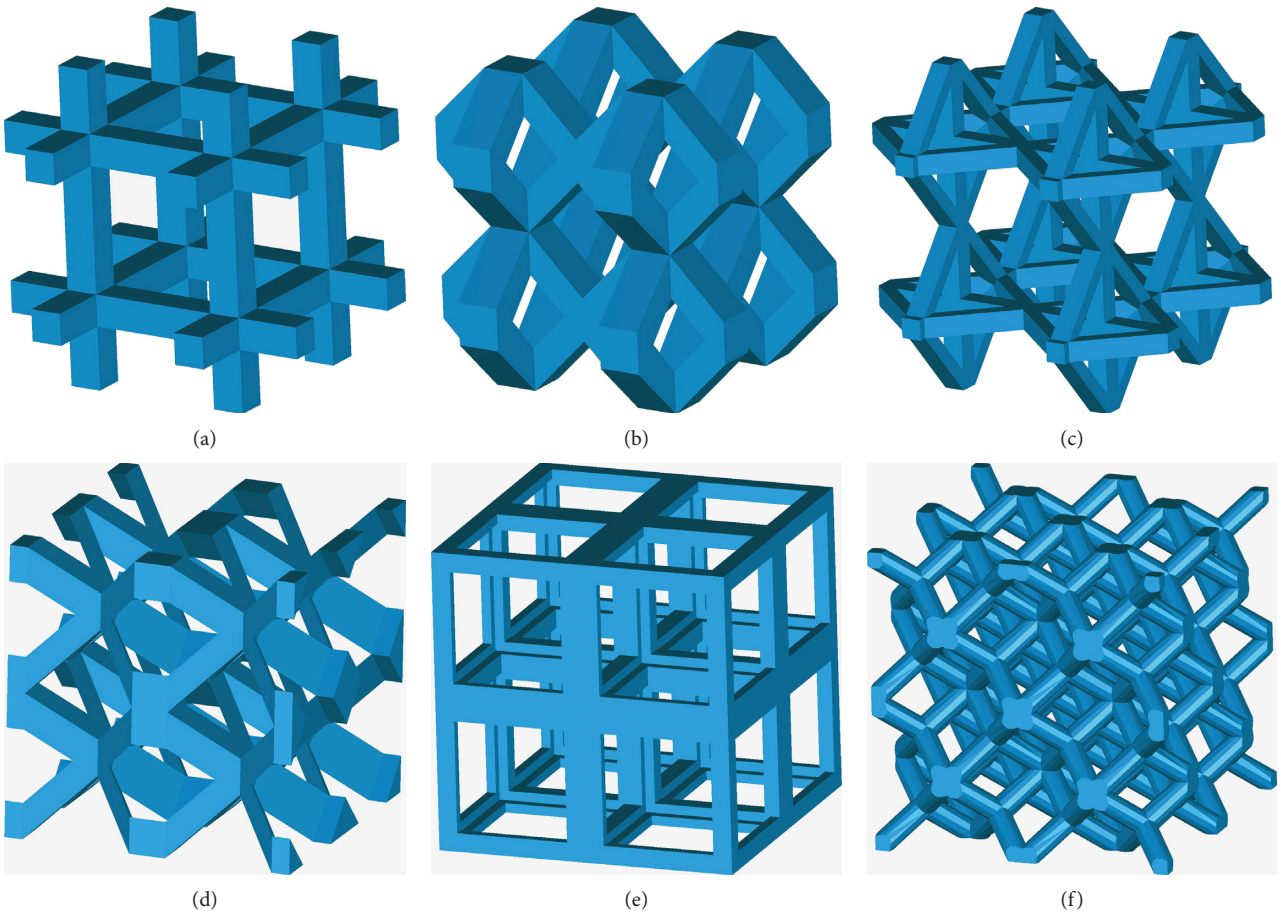

Figure 2: Diagram of the classic lattice structure: (a) cross cube; (b) FCC; (c) cross FCC; (d) BCC; (e) cube; (f) RD.

$$E_M = \frac{1}{N}\sum_{i=1}^{N} \xi E^H, \tag{9}$$

where N is the number of layers of the proposed model.

5. Realization of Multilevel Microstructure Filling

5.1. Multilevel Lattice Filling. Before the bionic design of multilevel organisms, a discrete grid data model of multilevel organism space must be obtained first, and then CT scan data are reconstructed for triangular grid data. The structures of organisms at all levels show gradient changes without unclear dividing line [19]. Optimizing the design accordingly is necessary to facilitate the later design after the reconstruction of the model in accordance with the actual situation. The structures of all levels are divided by clear boundaries through isosurface drawing, and the geometric parameter $\Omega_i (i \in N)$ is used to represent the space of all levels, where i is the number of biological levels. The dynamic parameters that need to be set at each level are entered, the matching lattice units are retrieved in the lattice database, and tile filling is performed.

5.2. Gradient Modeling Based on Level Set Method. The stability of the connection between lattice structures has a great effect on the macromechanics performance of multilevel structures. As shown in Figure 4(a), exactly matching the lattice structures is impossible. Enriching the lattice model family is necessary to solve this problem. However, exactly matching the alternative lattice structures is impossible [20]. Enriching the alternative lattice structures for the lattice model family is necessary, and a lattice with a higher matching degree coefficient ξ is selected to solve this problem. When retrieving lattice structures, then matching categories can be connected to each other, such as FBCC-BCC, FBCC-FCC, FBCC-FBCC, and FBCC-RD. Moreover, BCC and FCC cannot be directly connected, and FBCC has to be used as a transition lattice structure. The lattice is fused using an implicit surface-based method. Achieving uniform change in lattice gradient and improving the stability of numerical calculation are beneficial because the change rate of distance function is uniform. Figure 4(b) shows the effect of lattice fusion, and Figure 4(c) shows the effect of gradient change.

5.3. Performance Spatial Distribution. The OOFEM finite element library was used to perform structural modal analysis on the model, and then a multilevel mapping space

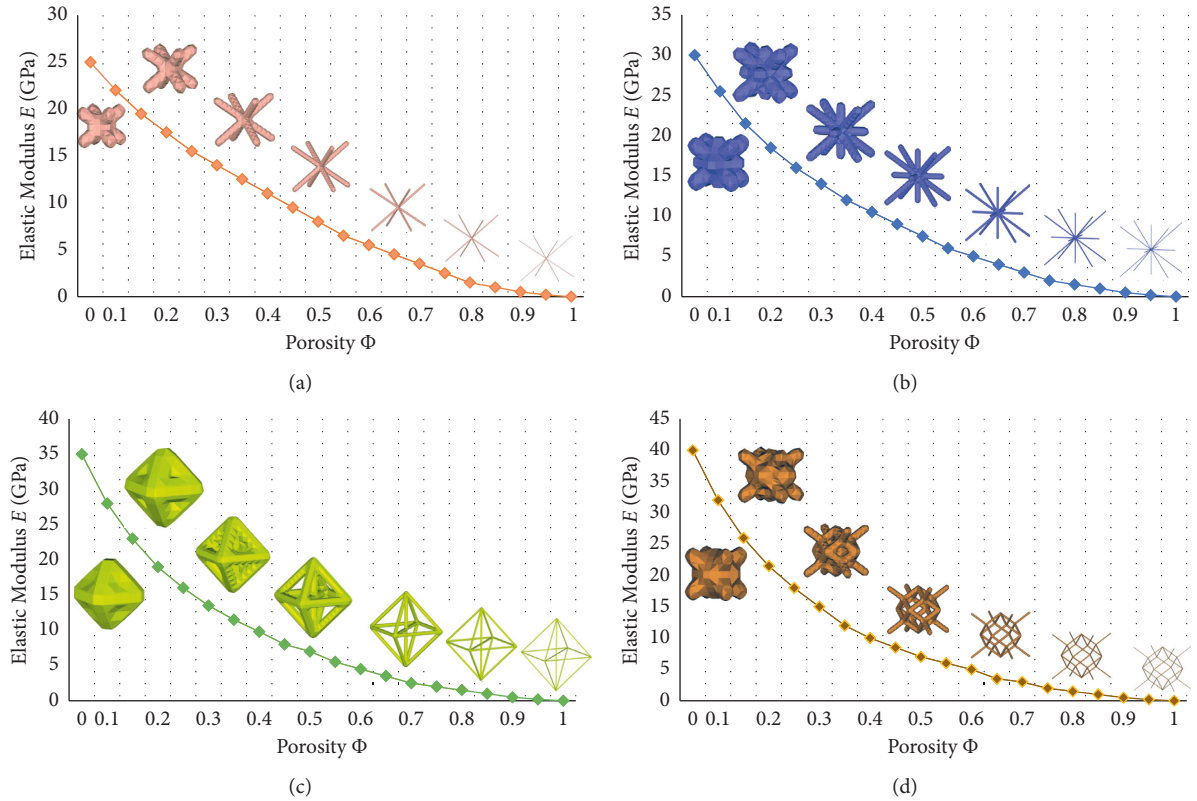

Figure 3: Elastic modulus corresponding to 3D lattice structure and different porosities: (a) BCC lattice; (b) FBCC lattice; (c) FCC lattice; (d) RD lattice.

was obtained Ω_i $(i \in N)$. The similar dynamic characteristic unit model $L_{i,j}$ $(i, j \in N)$ corresponding to different space Ω_i was selected through precomputation. The model space Ω_i was filled with the resulting unit structure $c_{i,j}$, and its relationship was demonstrated as

$$\Omega_i = \sum_{j=1}^{m} L_{i,j}. \tag{10}$$

A cylindrical workpiece with a length of 100 mm was used as an experimental object. A finite element simulation experiment was conducted to introduce the texture mapping principle based on finite elements. The structural modal analysis of the workpiece, as shown in Figure 5(a), was performed, and a modal displacement cloud diagram was obtained, as shown in Figure 5(b). On the basis of a global contrast-based retention conversion method, the following parametric conversion functions were constructed:

$$\begin{aligned} I &= f(c, s), \\ c &= (r, g, b), \end{aligned} \tag{11}$$

where r, g, and b are the color vectors of each pixel and s is the saliency of the pixel. The colored modal displacement cloud map is converted to grayscale, and a good grayscale map is maintained, as shown in Figure 5(c). On the basis of the principle of gradient deformation, the mapping relationship between the displacement cloud map grayscale value and the model gradient O_{solution} was constructed.

$$G(I) = O_{\text{solution}}. \tag{12}$$

The gradient change in the lattice bar diameter was tuned and adjusted in accordance with different grayscale values in order to match the size of the different deformation amplitudes, as shown in Figure 5(d).

6. Experimental Analysis

6.1. Pressure Test. We conducted physical experiments and mechanics simulation experiments on multilevel lattice structures from several angles, such as arrangement combination, direction, and porosity, and compared the experimental results with the simulation results [21]. This process was performed to verify the effectiveness of multilevel microstructure in regulating elastic modulus parameters. As shown in Figure 6(a), three sets of comparative experimental samples were manufactured using polylactic acid material on the basis of fused deposition modeling. The arrangement of the three sets of multilevel lattice structural units is FBCC-RD-FCC, FCC-RD-BCC, and BCC-RD-FBCC. Each set was designed with 6 units, the rod diameter was changed evenly from 0.45 mm to 0.20 mm, and each multilevel unit structure consisted of $3 \times 3 \times 3$ single-level unit structure. During the structural test, an FR-1001C universal material testing machine was used for pressure testing, as shown in Figure 6(b). Before the experiment, a preload was applied to the model to present the lattice, and then the test was performed at a rate of 0.8 mm/min.

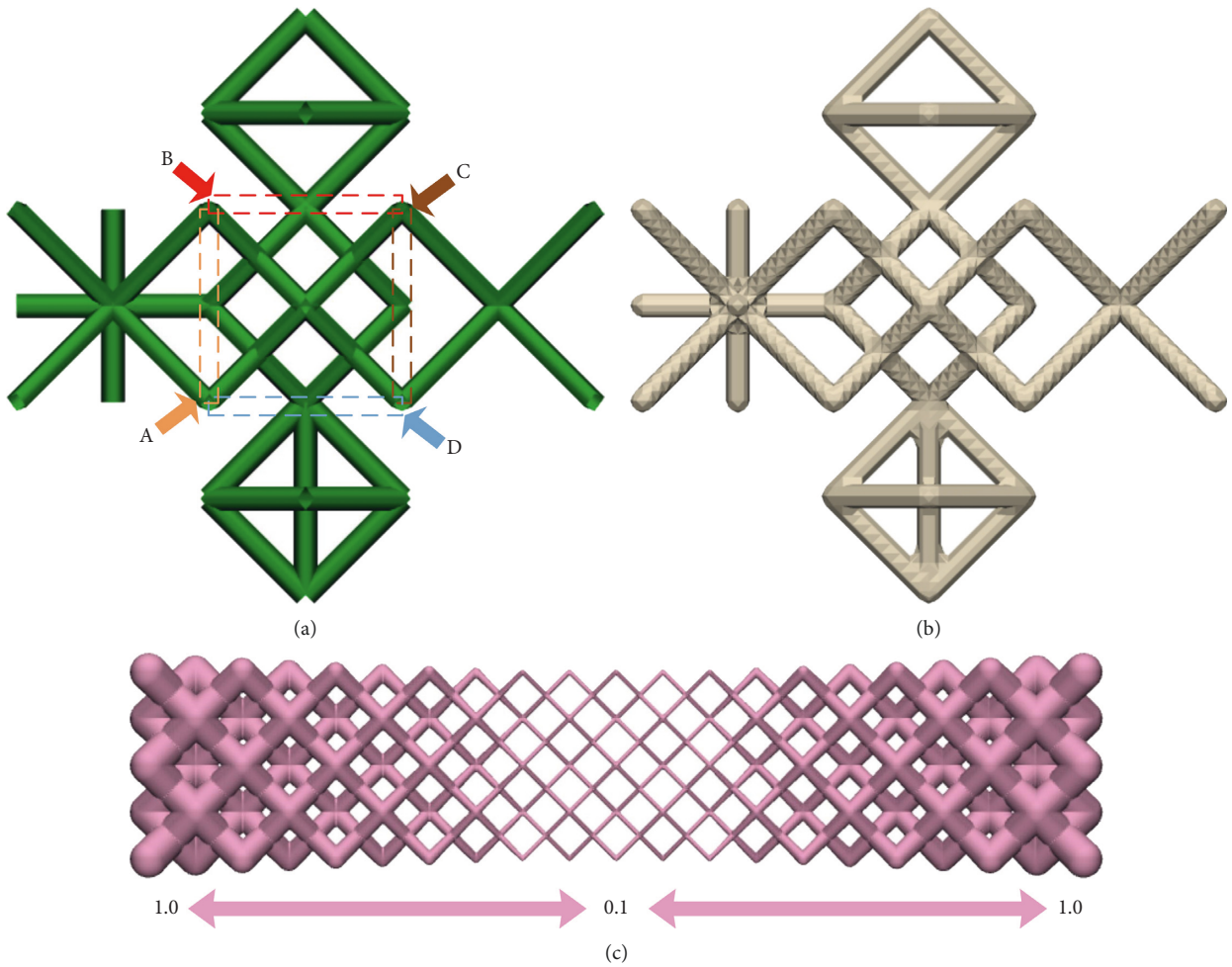

FIGURE 4: Fusion and gradient changes of unit lattices: (a) connection of common lattices; (b) the structure after lattice fusion; (c) gradient changes of lattice rod diameter from 1.0 mm to 0.1 mm.

The linear part of the stress-strain curve for the stress test was linearly fitted. Figure 7 shows a fitted effect diagram of the elastic modulus of the FCC-RD-FBCC structure. The solid line represents the numerical change in the real stress-strain curve, and the imaginary slope of the fitted dotted line is the value of the elastic modulus.

Figure 8(a) shows the multilevel lattice structure BCC-RD-FCC. Given its anisotropy, forces from all directions may be applied in 3D space. The finite element simulation results are compared with the physical experiment results to ensure the consistency between the design results and the real force. The lattice is tested for pressure from the three directions of *A*, *B*, and *C*. Figures 8(b) to 8(d) show the results of three sets of simulations and physical experiments. As shown in Table 1, the fitting results of simulation and experiment results are in good agreement. Thus, the obtained results are feasible.

6.2. Impact Test. A total of 24 test samples (80 mm × 10 mm × 6 mm) that were categorized into 4 various sets were manufactured through the well-known photocuring forming process. This should be noted that each sample has approximately 360 lattice units, and the sample rod diameter varies evenly between 0.5 and 1.5 mm. The impact resistance of the multilevel lattice unit, that is, the toughness of the lattice unit, was evaluated with a DELTA-TPO pendulum impact tester. The test temperature is set to 10 °C, and the shock energy of the pendulum is 25 J. The impact toughness a_k value of each set of models is recorded each time the angle of the pendulum is zeroed, and the sample is placed evenly [22].

The impact test results of the different types of lattice unit structures and different porosity rates are represented in Figure 9, and the test results are linearly fitted. As shown in Figures 9(a) and 9(b), the porosity of the FCC, BCC unit lattice structure, and multilevel lattice unit structure varies in waves between 0 and 1. As shown in Figure 9(c), the porosity of the RD unit varies linearly between 0 and 0.36. The test results, in fact, show and demonstrate good regularity as a whole. Although some errors are found in the impact toughness test results, they are controllable. These results provide an important design reference for the later design of object structures with different properties.

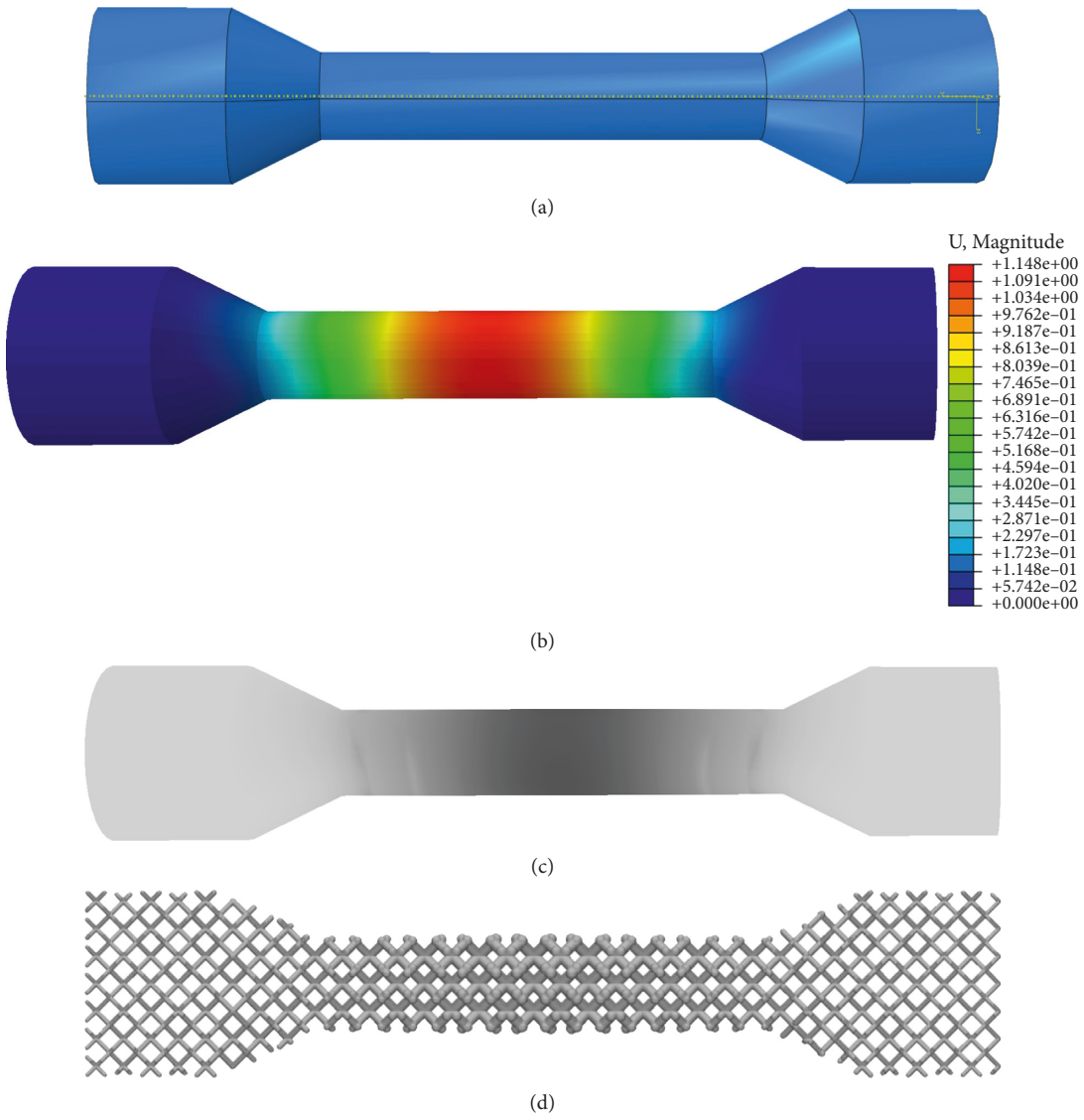

Figure 5: Finite element data mapping experiment: (a) cylindrical workpiece; (b) structural mode displacement cloud map; (c) grayscale map; (d) results of image mapping.

7. Multilevel Bionic Microstructure Design

A great deal of research is conducted on the elasticity, hardness, and fracture mechanical properties of enamel and dentin. Parameters, such as elastic modulus and hardness, are widely studied in the existing literature. The mechanical properties of different teeth are relatively different, and the third molars are the most abundant [23]. Thus, the third molars of adult males are selected as the research object. The elastic modulus of the multilevel structure composed of natural enamel, dentin, and dental pulp is taken as the main regulatory objective, which can help achieve the advantages of multilevel lattice structure. The hardness of the outer and the softness of the inner can highlight the toughness of the teeth.

The design of the multilevel tooth model is achieved mainly through the following steps (Figure 10). In accordance with the tooth CT slice, the three separate layer spaces of enamel layer, dentin layer, and dental pulp cavity layer are reconstructed, and they are represented as Ω_1, Ω_2, and Ω_3. Three lattices are selected in the middle of the lattice model family in accordance with the principle of lattice selection by setting the range of dynamic parameters of space at all levels (Table 2). The space at all levels is tiled and filled, as shown in Figure 10(c). The roots of the multilevel dental model are then fixed to simulate the binding of natural teeth by periodontal ligaments and alveolar bones, and vertical occlusal loads are applied, as shown in Figure 10(d). A cloud map of multilevel tooth stress field is obtained through finite element analysis, as shown in Figure 10(f). The stress on the left side of the enamel layer is concentrated [24]. Thus, reducing the lattice porosity, improving its hardness, and enhancing its antiwear cutting capacity are necessary.

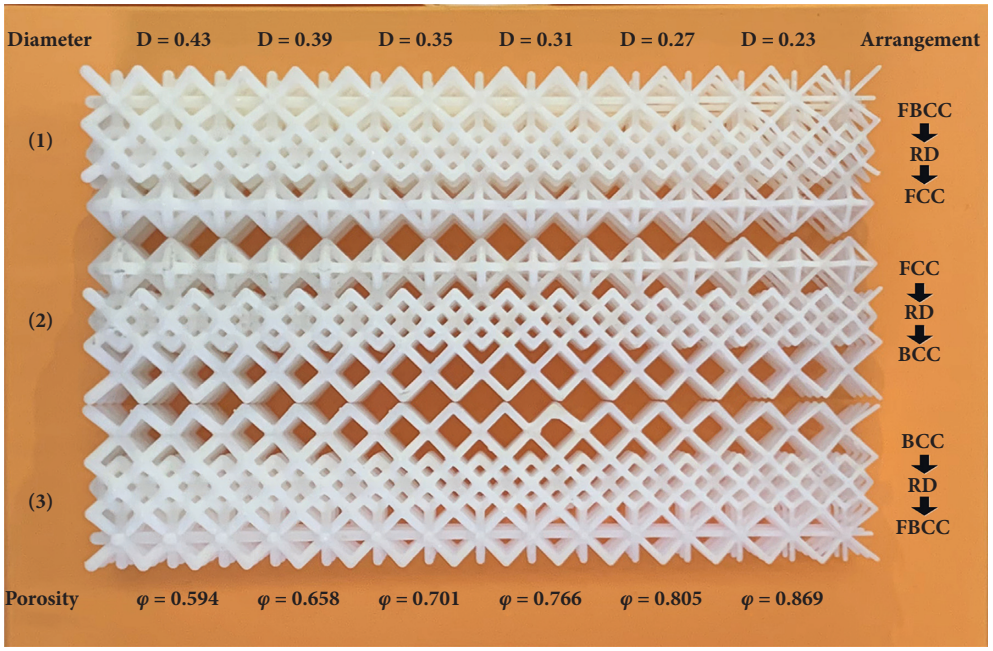

(a)

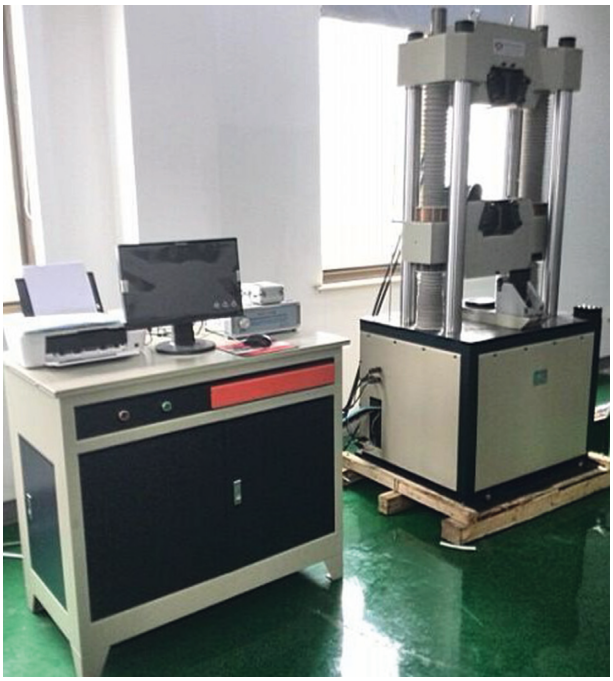

(b)

Figure 6: Multilevel lattice unit compression experiment: (a) multilevel lattice samples; (b) universal testing machine.

A certain phenomenon of stress concentration is observed at all connection levels. Thus, the lattice rod diameter for transition is larger to improve the ability to withstand stress concentration. The stress field cloud map is mapped to the multilevel lattice structure to obtain the multilevel lattice model with gradient changes [25]. The connection between the model levels is enhanced to ensure the effective transmission of force. The force is then changed between 50 and 450 N to determine whether the model deformation interval is within the maximum deformation range. The porosity of the lattice unit is adjusted in time to indirectly drive the change in the elastic modulus of the lattice at all levels to ensure that the actual hydraulic needs are met.

This should be noted that the entire model is iterated five times to produce the outcomes, as shown in Figures 10(c) and 10(h). The lattice unit with the outermost layer beyond

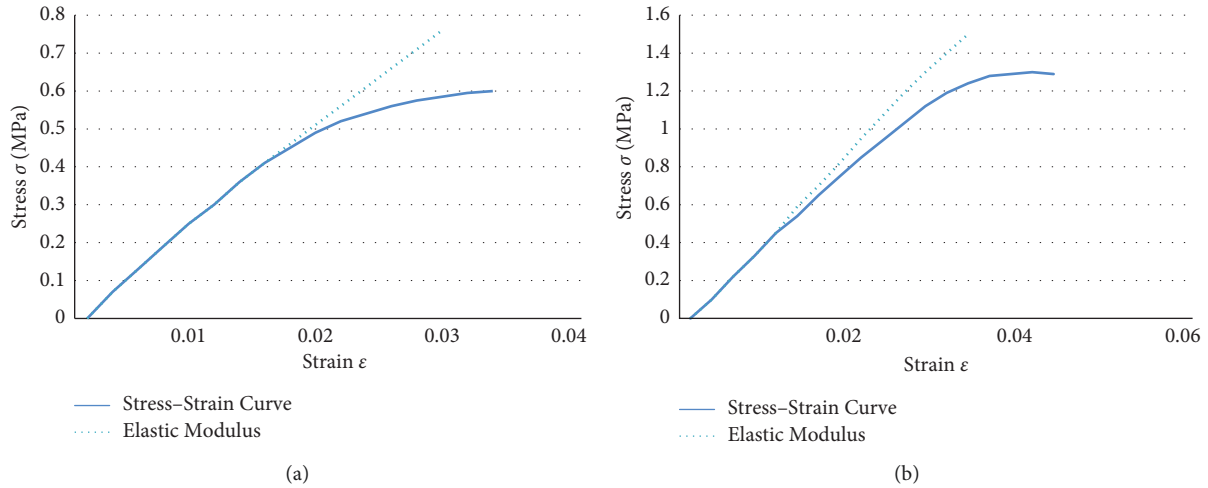

Figure 7: Stress-strain curve of FCC-RD-FBCC lattice structure with different porosities: (a)φ = 69.75%; (b)φ = 54.05%.

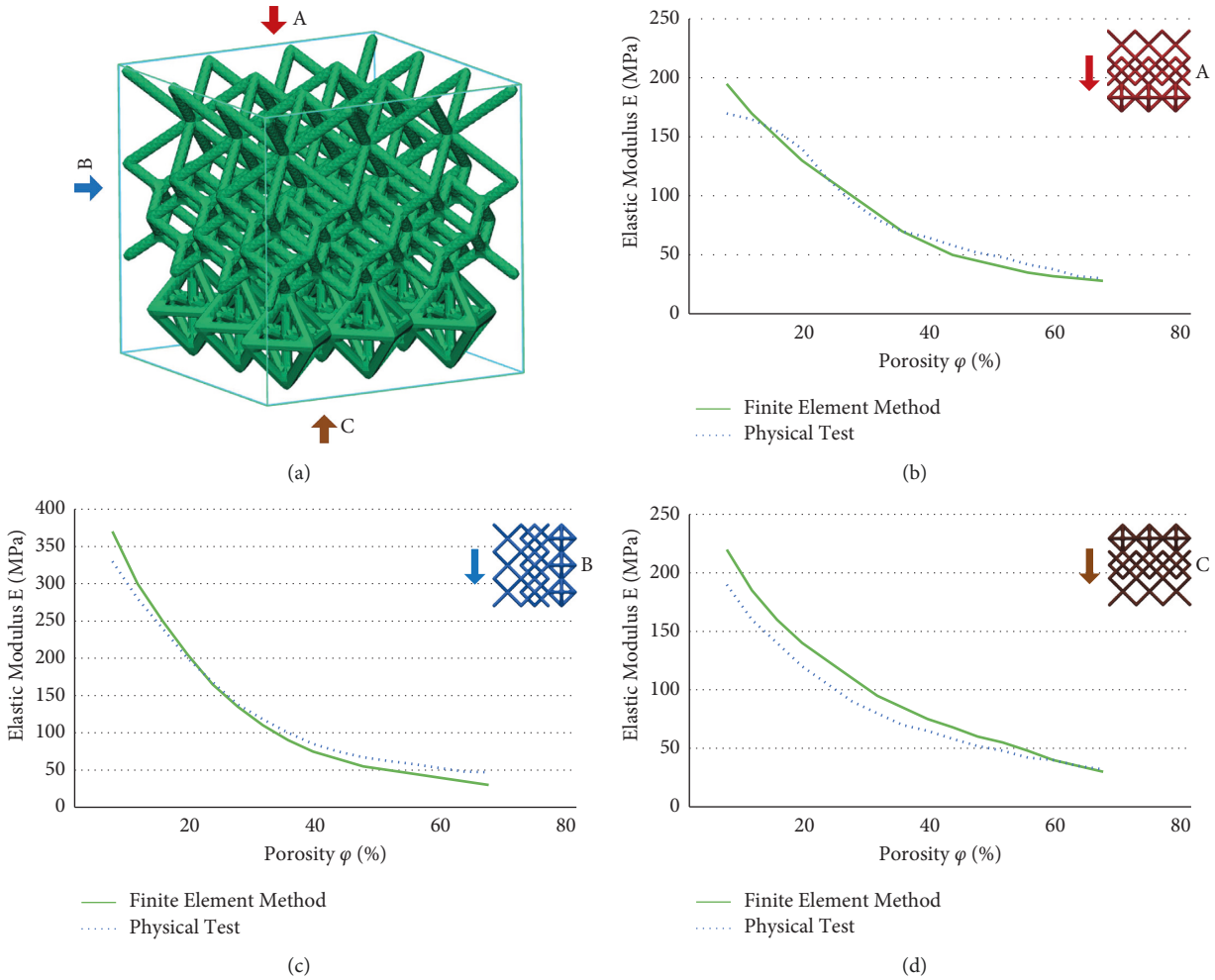

Figure 8: Comparison of three finite element simulation results with compression test data: (a) direction of force; (b) comparison of results in direction *A*; (c) comparison of results in direction *B*; (d) comparison of results in direction *C*.

the original boundary is cropped to obtain the result of Figure 10(g) and to ensure a desirable appearance. The resulting model is validated to ensure the validity of the design results, as shown in Figure 10(h). The obtained results demonstrate that the maximum fretting size of the resulting model is less than and close to the maximum fretting size of

Table 1: Similarity between the simulation results of the multilevel unit and the compression test data.

Direction of force	Direction A	Direction B	Direction C
Similarity (%)	91.12	87.91	86.77

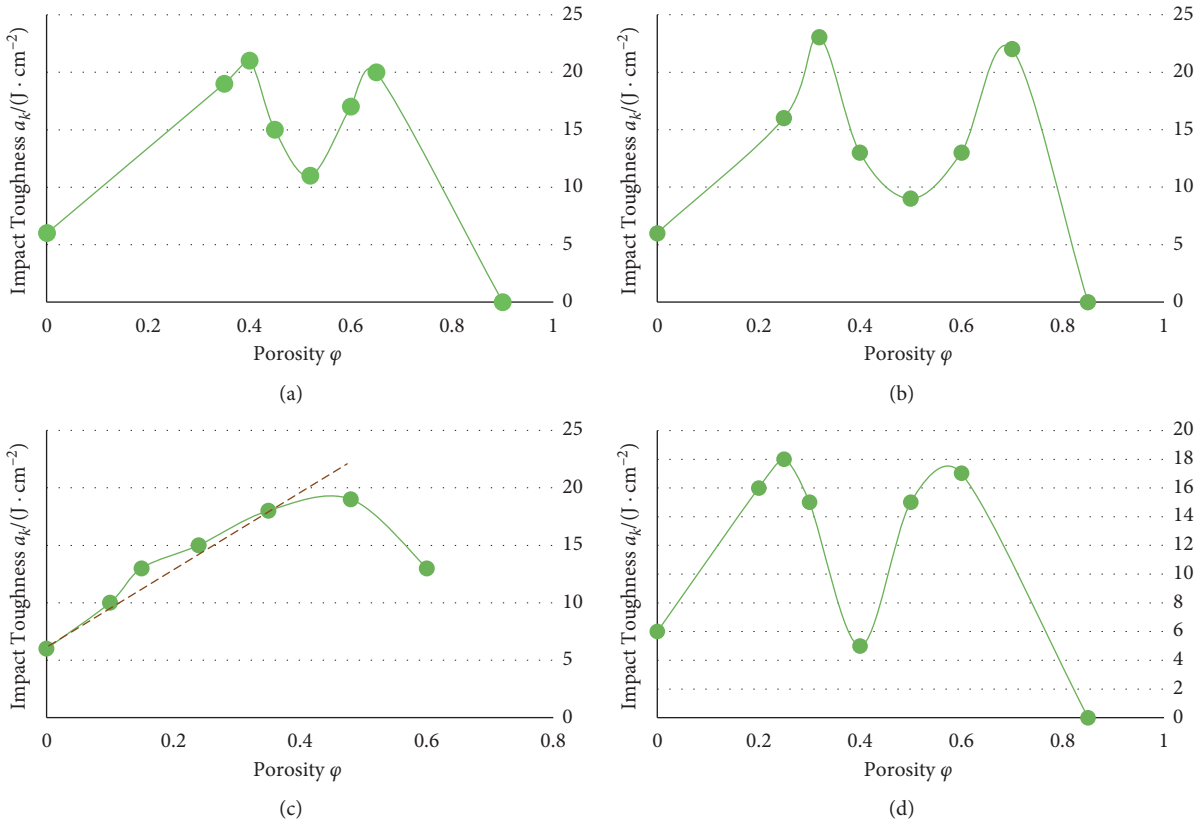

Figure 9: Impact test data of single-level and multilevel lattice units: (a) FCC lattice unit; (b) BCC lattice unit; (c) RD lattice unit; (d) multilevel lattice unit.

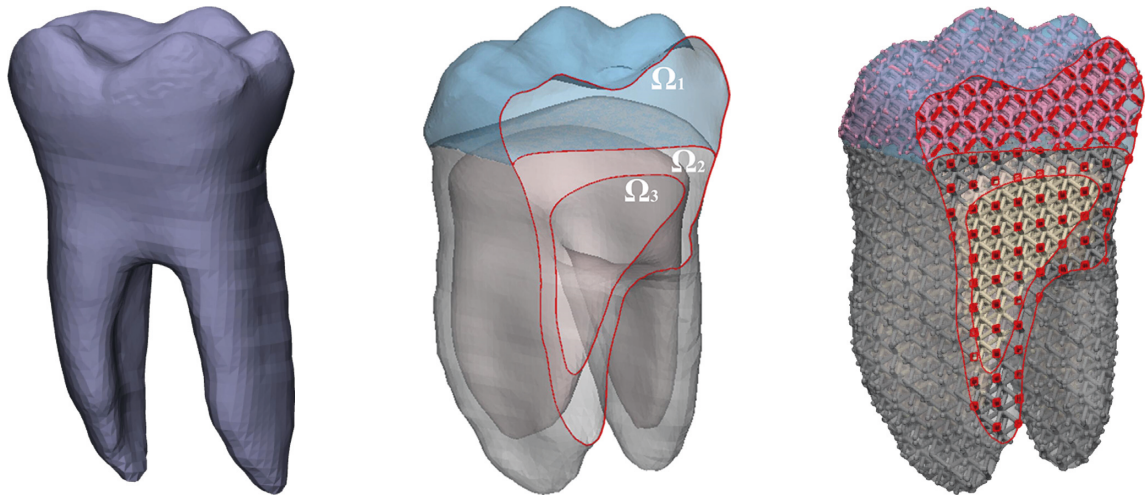

Figure 10: Continued.

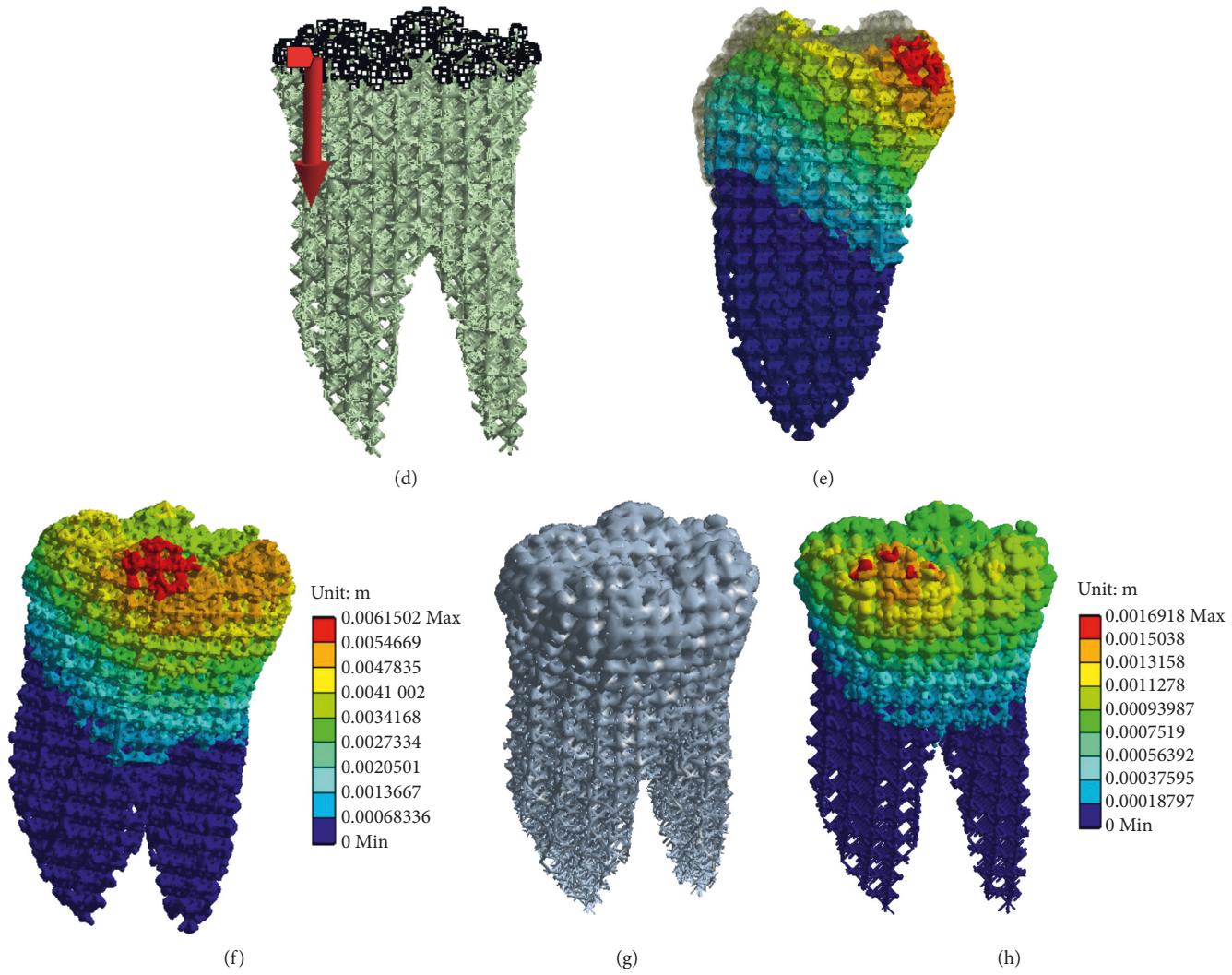

Figure 10: Bionic multilevel model simulation of molar: (a) model reconstruction; (b) 3D model cross sectional view; (c) lattice filling; (d) force and constraints imposed by finite element simulation; (e) deformation comparison; (f) displacement cloud diagram; (g) optimization model; (h) stress cloud diagram of the optimized model.

Table 2: Elastic modulus of molar tooth enamel and dentin.

	Measurement method	Elastic modulus (GPa)
Enamel	Nanoindentation	99.6 ± 1.8
Dentin	Nanoindentation	29.3 ± 6.7

the natural teeth (18.6 μm), thereby meeting the design requirements.

The proposed method can solve the problem of rigid connection between dental implants and periodontal bone. The resulting tooth model has a hard exterior layer and an internal structure that cushions deformation, thereby realizing the tough multilevel structure of the tooth and a porous structure. The porous structure is extremely beneficial to bone tissue growth. Over time, the connection between the implant and the periodontal bone becomes closer but not loose as traditional implants. In the above experimental discussion, we can clearly see and observe that the porous structure can effectively reduce the quality of the model, achieve lightweight, and better ensure the connection with surrounding bone tissues. This structure is conducive to growth and is biocompatible.

8. Conclusions and Future Work

In this study, we proposed the concept and geometric design method of multilevel lattice bionic microstructure modeling. The mechanical performance regulation of multilevel lattice structure and the diverse lattice connection and synthesis are realized. The efficiency of modeling is improved through preconstruction of microunit structure model families with different elastic moduli. Specific elastic modulus and impact toughness are obtained through finite element mapping, gradient change, and implicit surface fusion. The functional advantages of multilevel lattice structure are highlighted after applying the proposed technique to the modeling of biomedical prosthetic teeth. The resulting model has a hard external structure to resist damage and has a tough internal

structure to mitigate impact deformation, thereby achieving the biomechanical properties of tough structures. We observed that the porous structure can effectively reduce the quality of the model, achieve lightweight, and better ensure the connection with surrounding bone tissues. This structure is conducive to growth and is biocompatible.

In the future, we will further improve the proposed method so that it can solve the problem of rigid connection between dental implants and periodontal bone in an efficient and accurate way. To do so, we will consider larger datasets and artificial intelligence-based methods. Furthermore, as we identified earlier in this paper, over time, the connection between the implant and the periodontal bone becomes closer but not loose as traditional implants. Therefore, we will continue further research to investigate and design more robust lattice modeling methods along with gradient functions.

Data Availability

The data pertaining to this research are included for publication of this work.

Conflicts of Interest

The authors declare that there are no conflicts of interest regarding the publication of this paper.

Acknowledgments

This study was supported by the Scientific Research Foundation of Nanjing Vocational University of Industry Technology (YK18-03-03) and the Natural Science Foundation of the Jiangsu Higher Education Institutions of China (20KJB410005).

References

[1] X. Dong, H. Zhao, J. Li, and Y. Tian, "Progress in bioinspired dry and wet gradient materials from design principles to engineering applications," *iScience*, vol. 23, no. 11, Article ID 101749, 2020.

[2] J. B. D. Moreira, E. Lisboa, G. C. Rodrigues, F. B. Link, and W. J. B. Cases, "Multiscale topology optimization for frequency domain response with bi-material interpolation schemes," *Optimization and Engineering*, vol. 22, no. 4, 2020.

[3] J. P. Groen, C. R. Thomsen, and O. Sigmund, "Multi-scale topology optimization for stiffness and de-homogenization using implicit geometry modeling," *Structural and Multidisciplinary Optimization*, vol. 63, p. 7674, 2021.

[4] P. Liu, Y. Yan, X. Zhang, and Y. Z. Luo, "Topological design of microstructures using periodic material-field series-expansion and gradient-free optimization algorithm," *Materials & Design*, vol. 199, Article ID 109437, 2021.

[5] V.-N. Hoang, P. Tran, V.-T. Vu, and H. Nguyen-Xuan, "Design of lattice structures with direct multiscale topology optimization," *Composite Structures*, vol. 252, Article ID 112718, 2020.

[6] T. Dos'Santos, A. Mcburnie, C. Thomas, and P. P. A. Comfort, "Biomechanical comparison of cutting techniques: a review and practical applications," *Strength and Conditioning Journal*, vol. 41, no. 4, pp. 40–54, 2019.

[7] H. Zhang, X. Ding, Q. Wang, and W. H. Ni, "Topology optimization of composite material with high broadband damping," *Computers & Structures*, vol. 239, Article ID 106331, 2020.

[8] Y. Dong, X. Liu, T. Song, and S. He, "Topology optimization for structure with multi-gradient materials," *Structural and Multidisciplinary Optimization*, vol. 63, no. 3, pp. 1151–1167, 2020.

[9] M. Shimoda and S. Tani, "Simultaneous shape and topology optimization method for frame structures with multi-materials," *Structural and Multidisciplinary Optimization*, pp. 1–22, 2021.

[10] M. He, X. Zhang, L. dos Santos Fernandez, and A. L. T. Molter, "Multi-material topology optimization of piezoelectric composite structures for energy harvesting," *Composite Structures*, vol. 265, no. 1, Article ID 113783, 2021.

[11] L. Alacoque, R. T. Watkins, and A. Y. Tamijani, "Stress-based and robust topology optimization for thermoelastic multi-material periodic microstructures," *Computer Methods in Applied Mechanics and Engineering*, vol. 379, no. 17, Article ID 113749, 2021.

[12] J. Jia, D. Da, C.-L. Loh, and H. S. J. Zhao, "Multiscale topology optimization for non-uniform microstructures with hybrid cellular automata," *Structural and Multidisciplinary Optimization*, vol. 62, no. 2, pp. 757–770, 2020.

[13] C. Woischwill and I. Y. Kim, "Multimaterial multijoint topology optimization," *International Journal for Numerical Methods in Engineering*, vol. 115, no. 13, pp. 1552–1579, 2018.

[14] V. Florea, M. Pamwar, B. Sangha, and I. Y. Kim, "3D multi-material and multi-joint topology optimization with tooling accessibility constraints," *Structural and Multidisciplinary Optimization*, vol. 60, no. 6, pp. 2531–2558, 2019.

[15] Y. Luo, J. Hu, and S. Liu, "Self-connected multi-domain topology optimization of structures with multiple dissimilar microstructures," *Structural and Multidisciplinary Optimization*, vol. 64, no. 1, pp. 125–140, 2021.

[16] P. Liu, Z. Kang, and Y. Luo, "Two-scale concurrent topology optimization of lattice structures with connectable microstructures," *Additive Manufacturing*, vol. 36, Article ID 101427, 2020.

[17] J. Tölke, S. Freudiger, and M. Krafczyk, "An adaptive scheme using hierarchical grids for lattice Boltzmann multi-phase flow simulations," *Computers & Fluids*, vol. 35, no. 8-9, pp. 820–830, 2006.

[18] L. Chen and R. T. Zhang, "Pore-scale study of effects of macroscopic pores and their distributions on reactive transport in hierarchical porous media," *Chemical Engineering Journal*, vol. 349, pp. 428–437, 2018.

[19] C. Wang and X. J. Gu, "Concurrent design of hierarchical structures with three-dimensional parameterized lattice microstructures for additive manufacturing," *Structural and Multidisciplinary Optimization*, vol. 61-3, no. 3, pp. 869–894, 2020.

[20] A. Ali, Y. Zhu, and M. Zakarya, "Exploiting dynamic spatio-temporal graph convolutional neural networks for citywide traffic flows prediction," *Neural Networks*, vol. 145, no. 2022, pp. 233–247, 2022.

[21] A. Ali, Y. Zhu, and M. Zakarya, "A data aggregation based approach to exploit dynamic spatio-temporal correlations for citywide crowd flows prediction in fog computing," *Multimedia Tools and Applications*, vol. 80-20, no. 20, Article ID 31401, 2021.

[22] D. Lyu, H. Fan, and S. Li, "A hierarchical multiscale cohesive zone model and simulation of dynamic fracture in metals," *Engineering Fracture Mechanics*, vol. 163, pp. 327–347, 2016.
[23] W.-X. Ma and X.-X. Xu, "Positive and negative hierarchies of integrable lattice models associated with a Hamiltonian pair," *International Journal of Theoretical Physics*, vol. 43, no. 1, pp. 219–235, 2004.
[24] H. Maeyama and T. J. N. Imamura, "Unsteady aerodynamic simulations by the lattice Boltzmann method with near-wall modeling on hierarchical Cartesian grids," *Computers & Fluids*, vol. 233, no. 2022, Article ID 105249, 2022.
[25] L. Zhang and Z. M. Y. S. Hu, "Hierarchical sheet triply periodic minimal surface lattices: design, geometric and mechanical performance," *Materials & Design*, vol. 209, no. 2021, Article ID 109931, 2021.